Supporting Information

Crucial Gating Residues Govern the Enhancement of Peroxygenase Activity in an Engineered Cytochrome P450 O-Demethylase

Panxia Zhao, [‡ a,c] Yiping Jiang, , [‡ a,b,c] Qian Wang, [‡ a] Jie Chen, [a,b,c] ,Fuquan Yao [a,b,d], and Zhiqi Cong [* a,b,c,d]

a CAS Key Laboratory of Biofuels and Shandong Provincial Key Laboratory of Synthetic Biology Qingdao Institute of Bioenergy and Bioprocess Technology, Chinese Academy of Sciences Qingdao, Shandong, P. R. China E-mail: congzq@qibebt.ac.cn
b Shandong Energy Institute, Qingdao, Shandong, 266101, P. R. China
c University of Chinese Academy of Sciences (UCAS) Beijing 100049, P. R. China
d Qingdao New Energy Shandong Laboratory Qingdao, Shandong, 266101, P. R. China

Contents

Experimental Procedures

Materials

The substrates, products and standards used were purchased from Sigma, TCI, Macklin, Aladdin, Bide and Ark. All conventional reagents were analytically pure, purchased from Shanghai Sinopharm Co. Ltd. or Tianjin Fuyu Fine Chemical Co. Ltd. and used as received without further processing.

Expression and purification of cytochrome P450 enzymes

The pET-28a (+) vectors containing CYP199A4 variants were transformed into Escherichia coli BL 21(DE3) cells, and the cells were cultivated in LB medium containing 50 μg/ml kanamycin. The cultures were grown at 37 °C with vigorous shaking (~200 rpm). When the OD 600 of the cultures reached 0.8~1.0, the temperature was cooled to 25 °C, and the expression was induced by the addition of IPTG (1 mM) and δ-aminolevulinic acid hydrochloride (0.5 mM). Following 16-20 h of expression, the cells were harvested by centrifugation and stored at -20 °C [1].

Purification was done by Ni-NTA metal-affinity chromatography[2]. Cell pellets were resuspended in ice-cold buffer A (100 mM KPi, 100 mM NaCl, imidazole (20 mM), pH 7.4) and lysed by sonication. Cell debris was removed by centrifugation for 30 min at 20 000 g, and the crude cell extraction were applied to a 5 mL bed volume column pre-equilibrated with buffer A. Nonspecifically bound proteins were washed from the column with 5 column volumes of buffer A containing 30 mM imidazole. The bound protein was eluted with buffer B (100 mM KPi, 100 mM NaCl, imidazole (200 mM), pH 7.4). The purified protein solution was exchanged with buffer C (100 mM KPi, 100 mM NaCl, pH 7.4), enzyme its variants concentrated by ultrafiltration and frozen in buffer C plus 50 % glycerol at -20 °C. The F182A, F182A/K89A, F182A/P90A, F182A/F185A, F182A/S247G, F182A/F298S and F182A/V355A mutations of the CYP199A4 peroxygenase have been reported previously[3]. The purified protein solution was exchanged with buffer C (50 mM Tri-HCl pH 7.4). CYP199A4 and its variants fractions were checked for purity by SDS-PAGE (Figure S1A), concentrated by ultrafiltration and frozen in buffer C plus 50 % glycerol at -20 ºC. Purified proteins were characterized by SDS page.

The formation of a ferrous CO complex was confirmed by UV-visible spectral change through the reduction of ferric heme of the wild type P450 and its mutants by addition of $Na_2S_2O_4$ in the presence of carbon monoxide (CO) (Figure S1B)[2].

The concentrations of CYP199A4 variants were measured by Hemochrome binding assay[4].A pyridine solution was made by combining pyridine (1.75 mL) and 1 M aqueous of NaOH (0.75 mL). The solution was mixed at room temperature then centrifuged for 30 s at 5000 rpm to remove excess aqueous base. To a cuvette containing 0.75 mL of protein solution in phosphate buffer (0.1 M, pH 8.0), 0.25 mL of the pyridine solution was added followed by 2 mg of sodium dithionite. A UV/vis spectrum was recorded immediately. Hemoprotein concentration was determined from the absorbance of the hemochrome complex using extinction coefficients of ε418 = 196 mM^{-1} cm^{-1}. Absorbance was assigned as the difference between the peak max at 418 nm and the baseline at 420 nm as determined by extrapolating from two points on either side of the hemochrome peak (390 nm and 450 nm).

Mutagenesis and recombination

All the mutations were made by PCR based site-directed mutagenesis, and the PCR-amplified target DNA fragments were assembled by kinase-ligase. The target mutant assembly products were then transformed into chemically competent *Escherichia coli* BL21(DE3) cells. Single colonies from the transformation plates were picked and cultured overnight at 37 °C with kanamycin (50 μg ml^{-1}). Overnight cultures were further sequenced to confirm the mutations.

The double mutants of CYP199A4 were prepared used F182A as parent templates[3]. The primers used were as follows:

mutation	Sequence (5'--3')
D251A F	5'- GCAACGACCGTTAATGGCATTGGC -3'
D251A R	5'- CAGGCCGGCACTCAGCAGAC -3'
D251G F	5'- GCAACGACCGTTAATGGCATTGGC -3'
D251G R	5'- GGTACCACCGTTAATGGCATTGGC -3'
D251N F	5'- GCCTGAATACCACCGTTAATGGCATTGGCGCC -3'
D251N R	5'- AACGGTGGTATTCAGGCCGGCACTCAGCAGAC -3'
D251H F	5'- CCTGCATACCACCGTTAATGGCATTGGCGCCG -3'
D251H R	5'- TAACGGTGGTATGCAGGCCGGCACTCAGCAGA -3'
D251E F	5'- CCTGGAAACCACCGTTAATGGCATTGGCGCCG -3'
D251E R	5'- TAACGGTGGTTTCCAGGCCGGCACTCAGCAGA -3'

Protein Crystallization

For crystallization of CYP199A4 F182A in complex with 4-methoxybenzoic acid (4-MBA), the affinity column-purified protein was subjected to gel filtration using a HiPrep 16/60 Sephacryl S-200 column (Cytiva), followed by concentration and storage in a 50 mM Tris buffer (pH 7.4) prior to crystallization. Crystallization was carried out at 18 °C using the hanging drop evaporation method by mixing 1 µL protein solution (40 mg/mL protein supplemented with 1 mM 4-MBA) and 1 µL reservoir solution (0.1 M bis-Tris, 0.2 M Mg $(Ac)_2$ and 27 % PEG 3350, pH 5.5). Sword-like single crystals were obtained within three weeks and cryo-protected with the mother liquor supplementation of 20 % glycerol before being transferred into liquid nitrogen for data collection.

Data Collection and Structure Determination

X-ray diffraction data of CYP199A4 F182A in complex with 4-MBA were collected on BL19U1 beamline at the Shanghai Synchrotron Radiation Facility (SSRF) with a DECTRIS PILATUS3 6 M detector at 100 K and processed with Aquarium[5]. The structure was solved by molecular replacement with PHENIX Phaser-MR[6], using our previously determined structure of CYP199A4 F182T (PDB ID: 8HGC) as the search model.[3] The structural model was further built using COOT[7] and refined by PHENIX Refine[8]. The overall quality of the structure was checked by MolProbity[9] and deposited in the Protein Data Bank (PDB ID: 8WS4). Data collection and refinement statistics are shown in Table S1. Protein structure graphics were generated by PyMOL (https://www.schrodinger.com).

Simulation Method

The protonation of enzymes was calculated at pH 7.4 using the online server H++[10, 11]. All models were built using Gromacs 2023[12]. The AMBER-ff19SB force field[13] was used for enzymes. Structure optimization and frequency analysis of heme, ligand and H_2O_2 were performed using ORCA 5.0.4[14]. The force field parameters of these molecules were then obtained, and topology files were generated using both Multiwfn[15] and AmberTools[16, 17]. All parameters of atom types were fitted using GAFF, except for Fe atoms, which were fitted using UFF[18] The TIP3P water model was used to construct a cubic water box to solvate the systems, and ions were added to maintain electrical neutrality. All simulations were performed with periodic boundary conditions.

All simulations were performed using the GPU version of Gromacs 2023, and pre-equilibrium simulations preceded all production phase simulations. In the pre-equilibrium stage, the steepest descent method was used to minimize energy. Under a constant pressure of 1 bar, the temperature was gradually heated from 0 K to the target temperature (303k) in 1000 ps and given sufficient time for relaxation. The equilibrium was ensured by monitoring the potential energy, temperature and density convergence of the system at each stage. The SETTLE algorithm[19] was used to constrain the structure of water, while the LINCS algorithm[20] was used to constrain the bonds connected to H atoms. The Particle Mesh Ewald (PME) algorithm[21] was used to estimate the long-range electrostatic interactions. The V-rescale algorithm was used to couple the temperature of the solute and solvent to achieve more accurate control, whereas the Berendsen algorithm[22] and Parrinello-Rahman algorithm[23] were used to couple the pressure of the system at NPT and the production phase, respectively.

Umbrella sampling is an effective method to calculate the free energy difference of biological systems[24]. In this study, one H_2O_2 was placed at the entrance to the tunnel as the molecule to be pulled, and the distance between H_2O_2 and the Fe atom was set as the reaction coordinate. H_2O_2 was slowly pulled by a distance of approximately 4.5 Å from the Fe atom within 500 ps by applying a harmonic potential, the magnitude of which was determined by the difficulty of passing to ensure a reasonable process. Umbrella sampling was then performed based on the trajectory. To ensure sufficient overlap between windows and adequate sampling, conformational windows were acquired at 1 ps intervals and simulations were performed for 1 ns for each window (251 ns in total), with a fixed force constant of 5000 kJ/mol/nm^2 for H_2O_2. The samples from all the windows were converted into the potential of mean force (PMF) using the weighted histogram analysis method (WHAM)[25] to obtain the free-energy profiles along the reaction coordinate.

General Procedure for Demethylation of Benzoic Acid Derivatives by H_2O_2-Dependent CYP199A4

CYP199A4 and its variants (1 µM) were transferred to a glass flask containing Tris-HCl buffer (50 mM, pH 7.4) and benzoic acid derivatives (2 mM, 2 % DMSO). The reaction mixtures were incubated in a water bath at 30 °C for 2 min, and the reaction was initiated by adding H_2O_2 (10 mM dissolved in the Tris-HCl buffer). The reactions were incubated in the water bath at 30 °C for 60 min. The reactions were stopped with 20 µL HCl (1 M). The reaction mixtures were quenched and extracted with 1 mL of ethyl acetate, and the organic phase was separated and dried with anhydrous sodium sulfate. One-hundred and fifty microliters of BSTFA/TMCS (99:1) was added to 150 µL samples, and this mixture was incubated in a metal bath at 75 °C for 30 min. The product was confirmed by gas chromatography (GC) using benzophenone as an internal standard (i.e., taking peak area integration) and corresponding authentic compounds as standards.

Stability of CYP199A4 peroxygenases in H_2O_2

The haem degradation kinetics of CYP199A4 and variants (F182A, F182T, F182A/D251N, F182A/D251E) were determined by dissolving the enzyme (2 µM), 4-methoxybenzoic acid (2 mM) and H_2O_2 (10 mM) in 50 mM Tri-HCl, pH 7. The absorbance of CYP199A4 and the mutant at 418 nm was measured using a UV spectrophotometer. The degradation rate (1/t) was obtained by fitting a curve of time t to the change in absorbance Abs at 418 nm:

Abs=A0+Aexp(-k_{obs}t) or Abs=A0+A1exp(-k_{obs1}t) + A2exp(-k_{obs2}t)

Long-time demethylation of 3-methyl-4-methoxybenzoic acid

F182A/V355A (1 µM) was transferred to a glass sample bottle containing 50 mM, pH 7.4 Tri-HCl, 3-methyl-4-methoxybenzoic acid (4 mM, dissolved in methanol) at 30 °C. The reaction was initiated by the addition of H_2O_2 10 mM, dissolved in 50 mM, pH 7.4 Tri-HCl). The reaction mixture was incubated at 30 °C for 5 h. The reaction was stopped by the addition of dilute 20 µL HCl (1 M) aqueous. The organic phase was extracted by ethyl acetate (1mL) and dried over anhydrous sodium sulphate. One-hundred and fifty microliters of BSTFA/TMCS (99:1) was added to 150 µL samples, and this mixture was incubated in a metal bath at 75 °C for 30 min. The product was confirmed by gas chromatography (GC) using benzophenone as an internal standard (i.e., taking peak area integration) and corresponding authentic compounds as standards.

Semi-preparatory scale synthesis of 3-methyl-4-hydroxybenzoic acid by CYP199A4

4 µM F182A/V355A was transferred to a glass flask containing 50 mL of 20 mM pH 7.4 Tri-HCl in buffer, 4 mM 3-methyl-4-methoxybenzoic acid (dissolved at 2 %) in DMSO and the reaction was initiated by the addition of 10 mM H_2O_2 and allowed to react at 4 °C for 1 h. 1 mL of the reaction solution was taken up and extracted with 1 mL of ethyl acetate, and the organic phase was dried with anhydrous sodium sulfate. The formation of 3-methyl-4-hydroxybenzoic acid was determined by gas chromatography.

The raw reaction mixture was extracted three times with ethyl acetate (50 mL × 3), dried over anhydrous sodium sulphate for the combined organic phase and concentrated by filtration. 3-Methyl-4-hydroxybenzoic acid was obtained by TLC (dichloromethane: ethanol = 9:1) as a powder (18.0 mg, 59 %).

Gas Chromatography

Product analysis was performed on a Shimadzu GC-2030 plus equipped with a DB-5HT column (length: 30 m; internal diameter: 0.25 mm; film thickness: 1.0 µm; Agilent), a flame ionization detector and an AOC-20i autosampler system. The analytical conditions were as follows.

For demethylation reactions of substrates (**1–10, 13, 14, 16** and **18–21**): splitting ratio, 1/9; temperature program: injector 330 °C, detector 330 °C, 100 °C oven for 1 min, then 15 °C/min gradient to 220 °C, 60 °C/min gradient to 330 °C for 2 min (total 15.83 min).

For demethylation reactions of substrates (**11, 12**, **15** and **17**): splitting ratio, 1/9; temperature program: injector 330 °C, detector 330 °C, 100 °C oven for 1 min, then 60 °C/min gradient to 210 °C, 5 °C/min gradient to 220 °C, 60 °C/min gradient to 330 °C for 2 min (total 13.67 min).

Product Analysis by GC-MS

The GC-MS analysis was performed on an Agilent 7890 series GC equipped with an Agilent4 5975C mass selective detector (Agilent Technologies, Little Falls, DE, USA) and a DB-5MS capillary column (30 m × 0.25 mm × 0.25 µm; Agilent).

The analytical conditions for reactions involving substrates (**1–9, 11–13, 15** and **16**) were: carrier gas, He; flow rate, 1.0 mL/min; inlet temperature, 300 °C; the oven temperature was initiated at 70 °C for 1 min, increased to 220 °C at a rate of 15 °C/min, 60 °C/min gradient to 330 °C for 2 min; transfer line temperature, 270 °C; ion source temperature, 230 °C.

The analytical conditions for reactions involving substrates (**10, 14, 17** and **18**) were: carrier gas, He; flow rate, 1.0 mL/min; inlet temperature, 300 °C; the oven temperature was initiated at 70 °C for 1 min, then 60 °C/min gradient to 210 °C, 5 °C/min gradient to 220 °C, 60 °C/min gradient to 330 °C for 2 min; transfer line temperature, 270 °C; ion source temperature, 230 °C.

Substrate Binding: Binding Titrations

For dissociation constant determination, 2 mL of 2 µM CYP199A4 F182A in 50 mM Tri-HCl, pH 7.4 and 0.5–2 mL aliquots of the substrate were added using UV detection from 10 mM or 100 mM stock solutions in ethanol. The maximum peak-to-trough difference (ΔA) in absorbance between 700 nm and 300 nm was recorded. Further aliquots of substrate were added until the peak-to-trough

difference did not change. The equilibrium dissociation constant (K_d) was obtained by fitting ΔA against the total substrate concentration [S] to a hyperbolic function[26]:

$$\Delta A = \frac{\Delta A_{max} \times [S]}{K_d + [S]} \quad (1)$$

where ΔA_{max} is the maximum absorbance difference. Several substrates exhibited tight binding, with K_d < 1 mM. In these cases, the data were fitted to the tight binding quadratic equation:

$$\frac{\Delta A}{\Delta A_{max}} = \frac{([E] + [S] + K_d) - \sqrt{\{([E] + [S] + K_d)^2 - 4[E][S]\}}}{2[E]} \quad (2)$$

where ΔA_{max} is the maximum absorbance difference and [E] is the enzyme concentration.

Supporting Figures

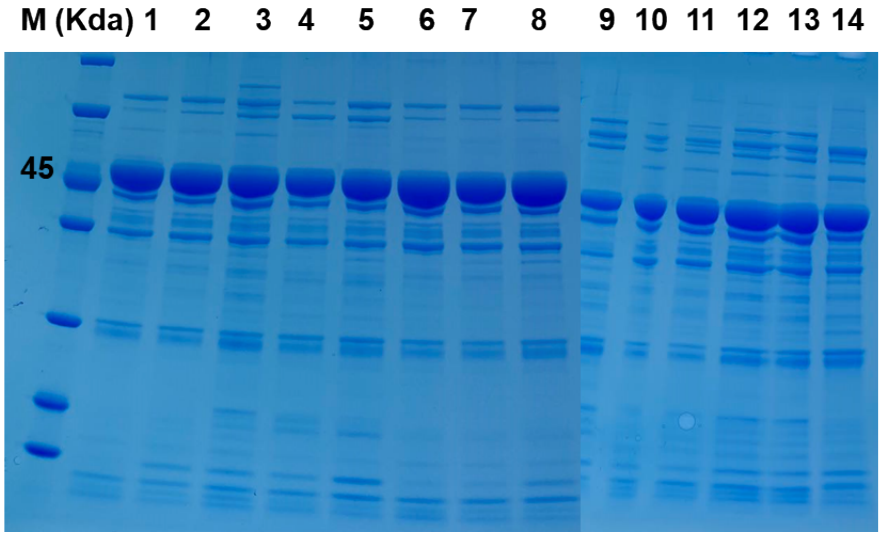

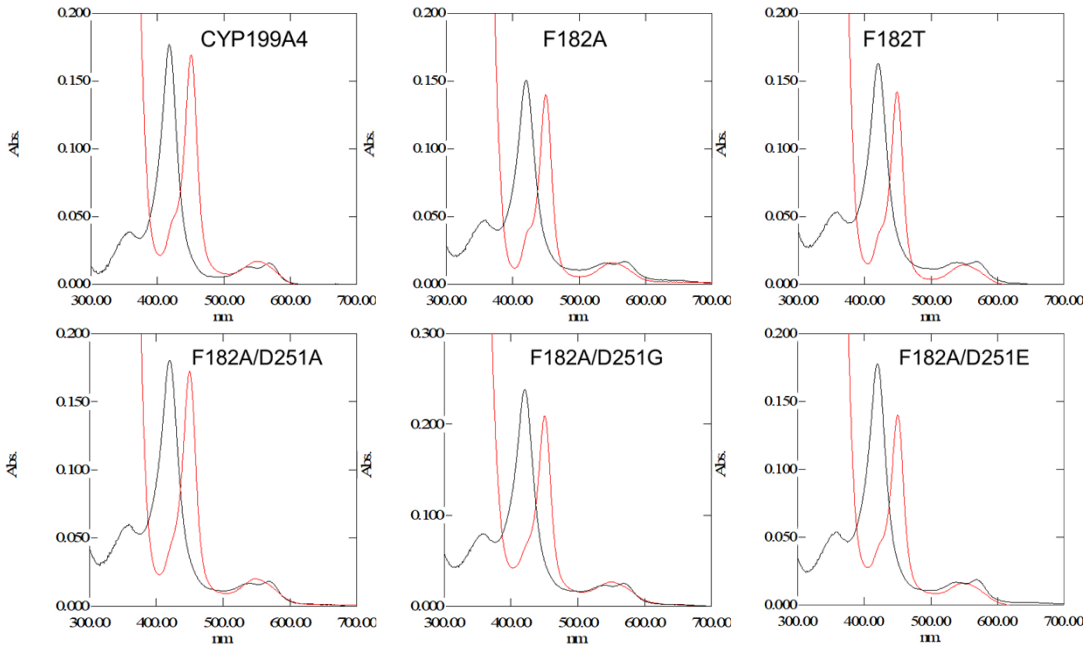

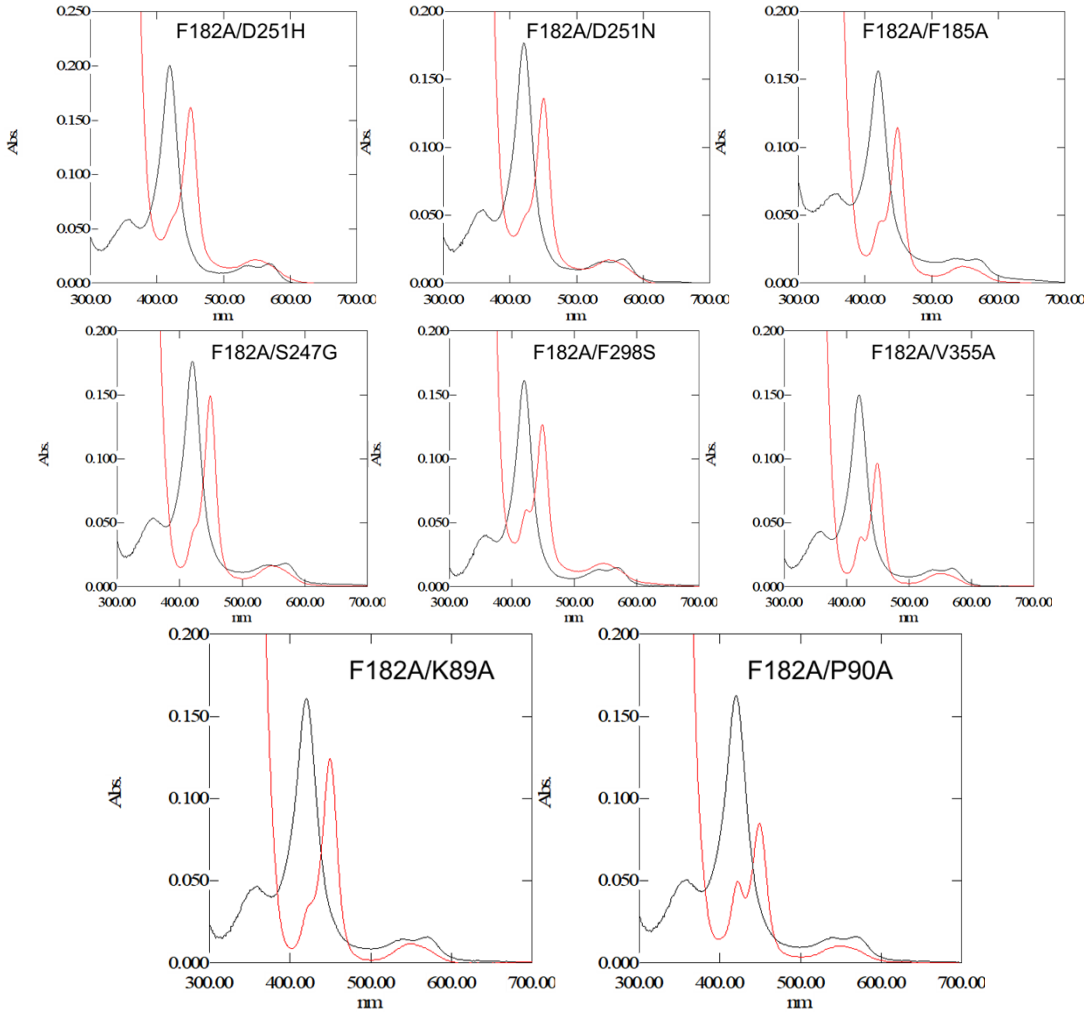

Figure S1. (A) SDS Page of CYP199A4 variants. Lane M:molecular standards；Lane A 1-14: CYP199A4, F182A.F182T, F182A/D251A, F182A/D251A, F182A/D251G, F182A/D251H, F182A/D251E, F182A/D251N, F182A/F185A, F182A/S247G, F182A/F298S, F182A/V355A, F182A/K89A, F182A/P90A; (B) UV/visible spectral changes of the typical variants (black line) upon addition of $Na_2S_2O_4$ (red line) for the formation of a ferrous CO complex through the reduction of ferric heme.

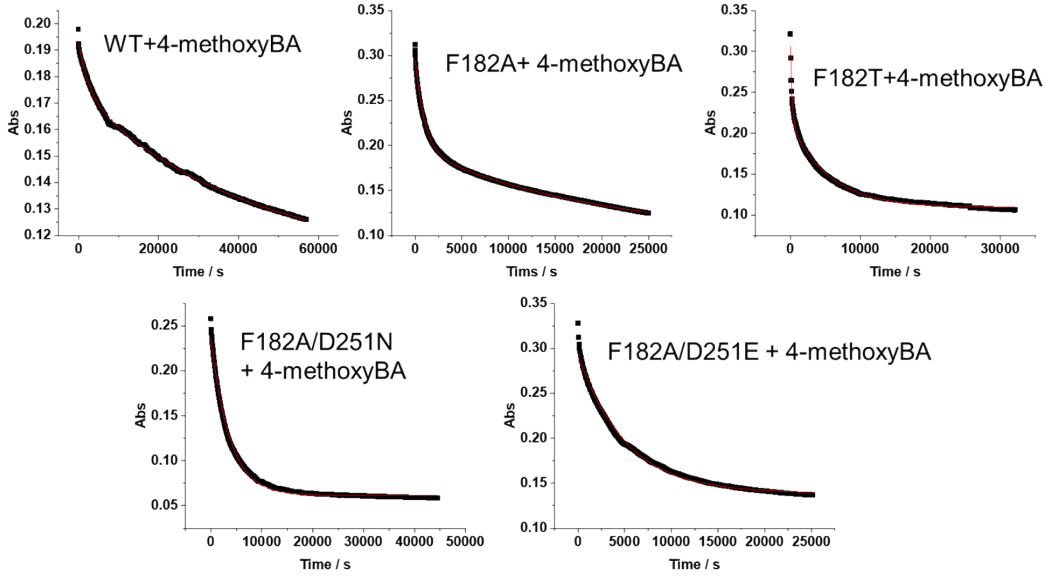

Figure S2. Determination of the kinetics of heme degradation in CYP199A4 and its mutants (F182A, F182T, F182A/D251N, F182A/D251E)，4-methoxyBA: 4-methoxybenzoic acid.

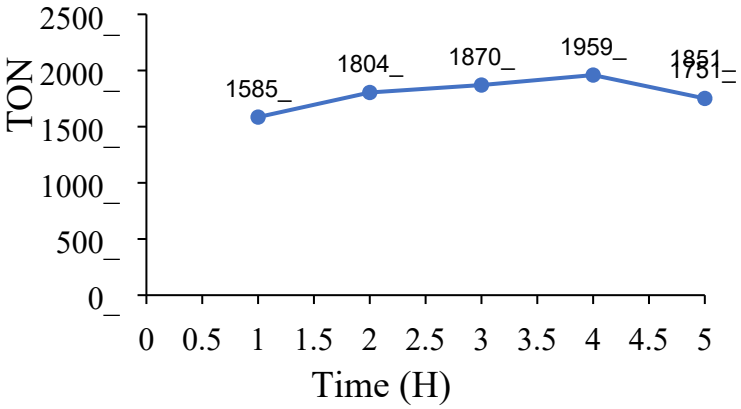

Figure S3. F182A (1 μM) catalyzes the long-term reaction of 4-methoxybenzoic acid at 30 °C in the presence of 10 mM H_2O_2.

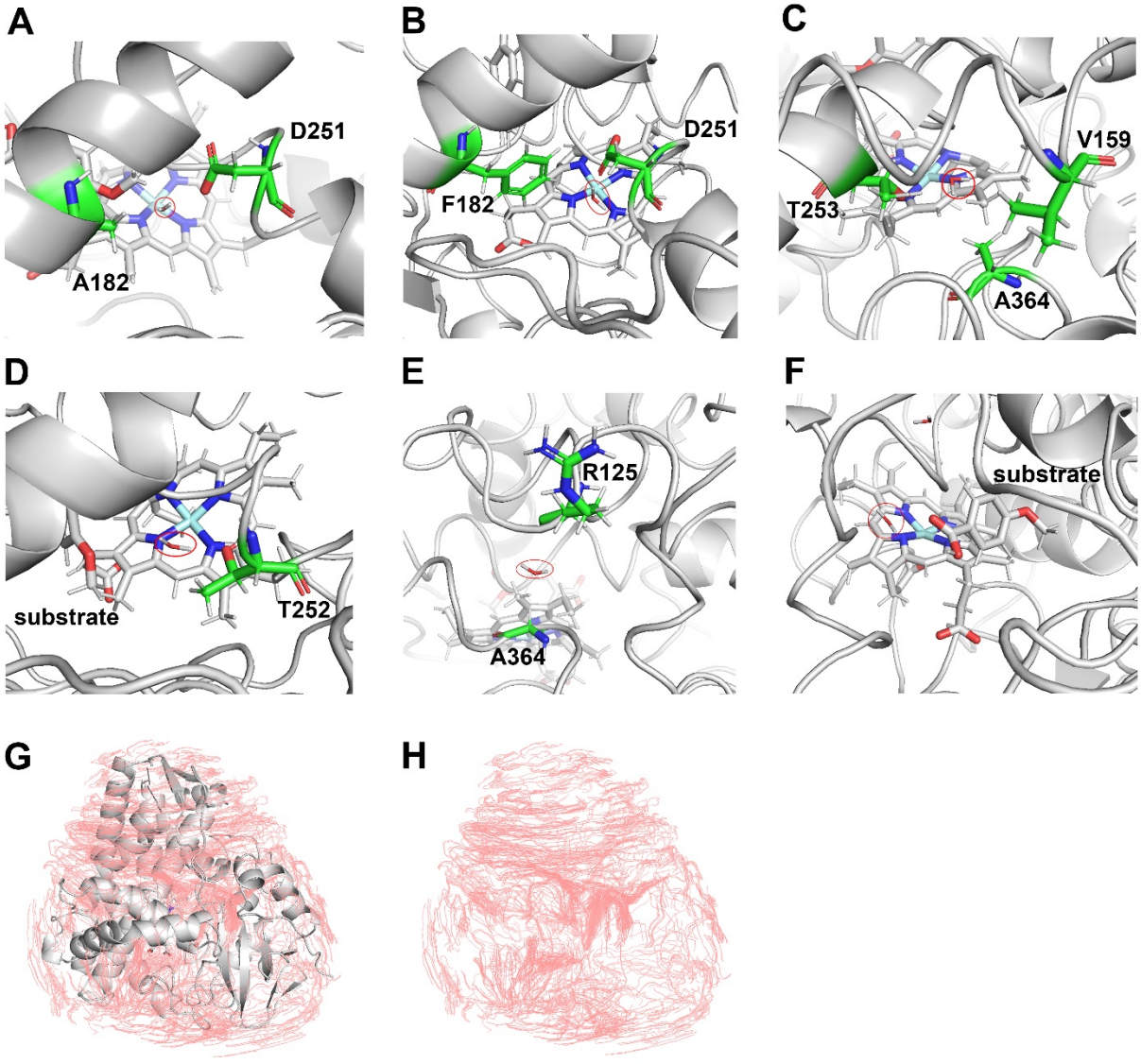

Figure S4. (A) The entry of the third H_2O into active site of F182A in 500ns. (B) The entry of H_2O into active site of wild type. (C) The entry of H_2O into active site of F182A/D251E. (D) and (E) The entry of H_2Os into active site of F182A/D251A; (F, G, H) The convergence of umbrella sampling simulations for wild-type CYP199A4, F182T and F182A, respectively. (I) and (J) The streamlines around and inside F182A with and without protein structure respectively.

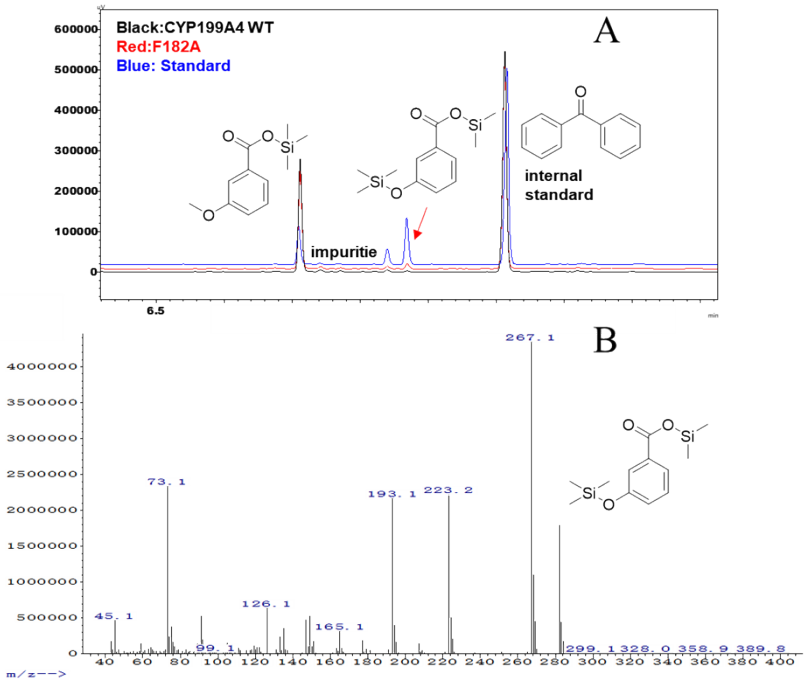

Figure S5. (A) GC analyses of the 60-minute reaction of 3-methoxybenzoic acid demethylation catalyzed by CYP199A4 WT and F182A (1 µM) at 30 °C in the presence of 10 mM H_2O_2. (B) GC-MS analyses for the product 3-Hydroxybenzoic acid (derivatized m/z= 312.5).

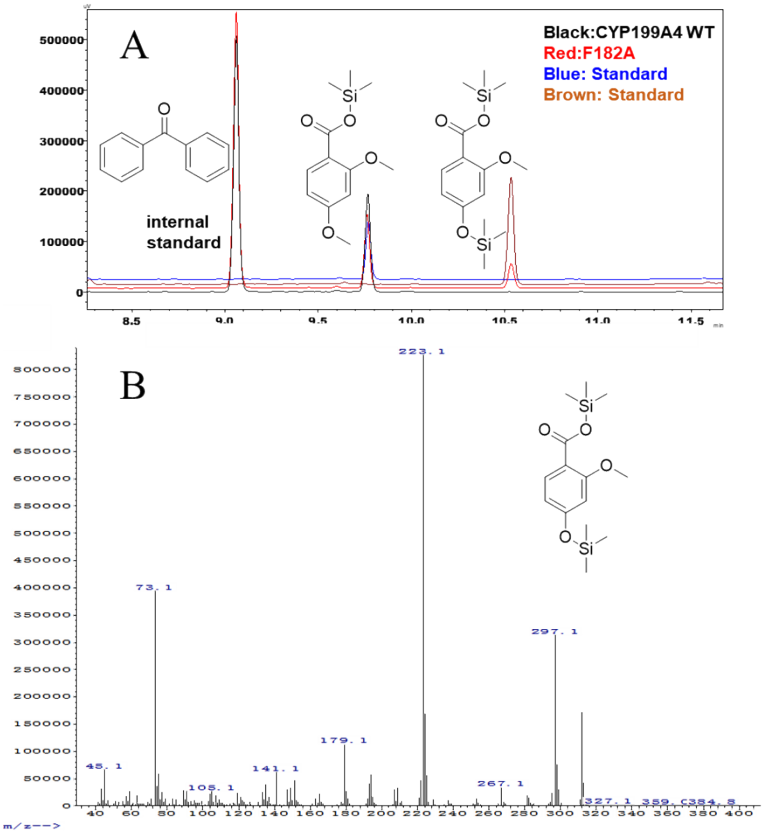

Figure S6. (A) GC analyses of the 60-minute reaction of 2,4-dimethoxybenzoic acid demethylation catalyzed by CYP199A4 WT and F182A (1 µM) at 30 °C in the presence of 10 mM H_2O_2. (B) GC-MS analyses for the product 2-methoxy-4-hydroxybenzoic acid (derivatized m/z = 312.5).

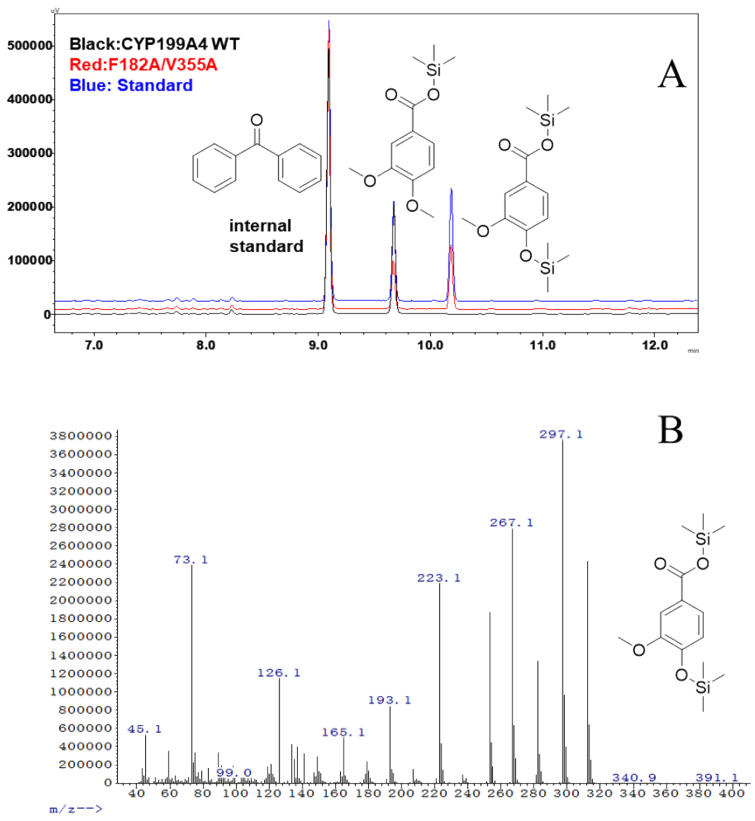

Figure S7. (A) GC analyses of the 60-minute reaction of 3,4-dimethoxybenzoic acid demethylation catalyzed by CYP199A4 WT and F182A/V355A (1 µM) at 30 °C in the presence of 10 mM H_2O_2. (B) GC-MS analyses for the product 3-methoxy-4-hydroxybenzoic acid (derivatized m/z = 312.5).

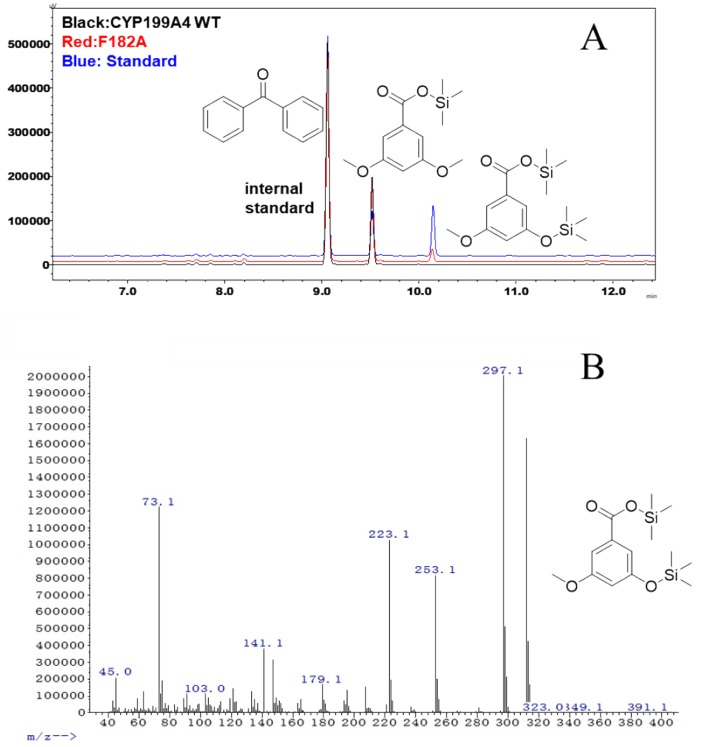

Figure S8. (A) GC analyses of the 60-minute reaction of 3,5-dimethoxybenzoic acid demethylation catalyzed by CYP199A4 WT and F182A (1 µM) at 30 °C in the presence of 10 mM H_2O_2. (B) GC-MS analyses for the product 5-methoxy-3-hydroxybenzoic acid (derivatized m/z = 312.5).

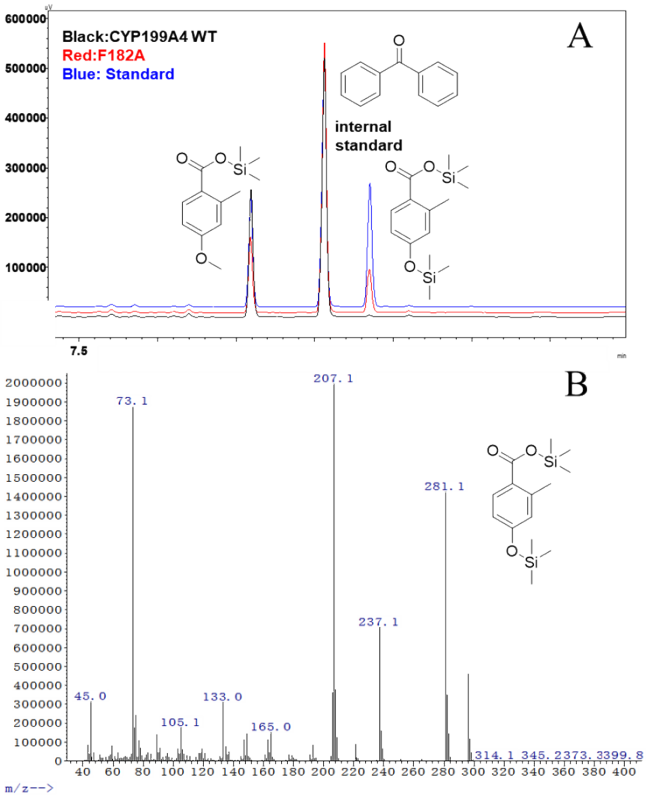

Figure S9. (A) GC analyses of the 60-minute reaction of 2-methyl-4-methoxybenzoic acid demethylation catalyzed by CYP199A4 WT and F182A (1 μM) at 30 °C in the presence of 10 mM H_2O_2. (B) GC-MS analyses for the product 2-methyl-4-hydroxybenzoic acid (derivatized m/z =296.1).

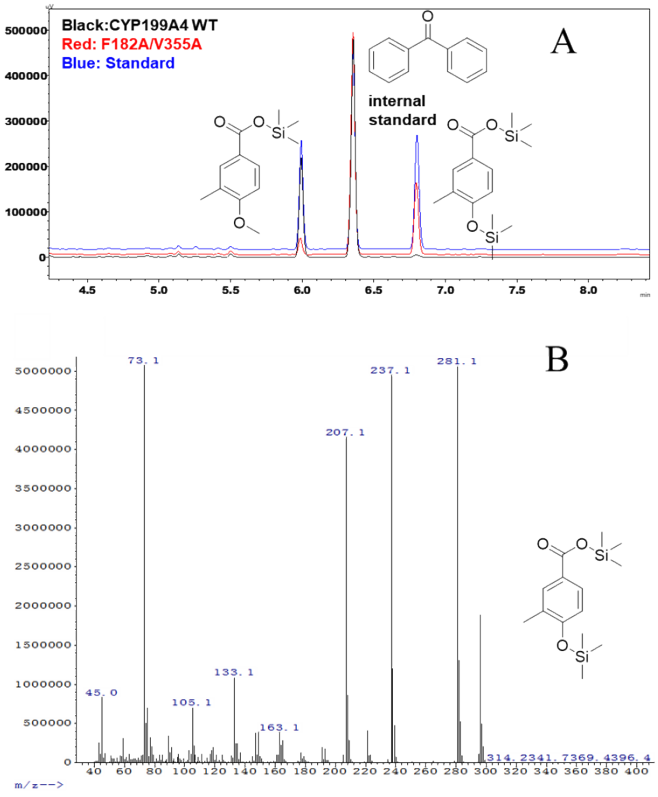

Figure S10. (A) GC analyses of the 60-minute reaction of 3-methyl-4-methoxybenzoic acid demethylation catalyzed by CYP199A4 WT and F182A/V355A (1 μM) at 30 °C in the presence of 10 mM H_2O_2. (B) GC-MS analyses for the product 3-methyl-4-hydroxybenzoic acid (derivatized m/z =296.1).

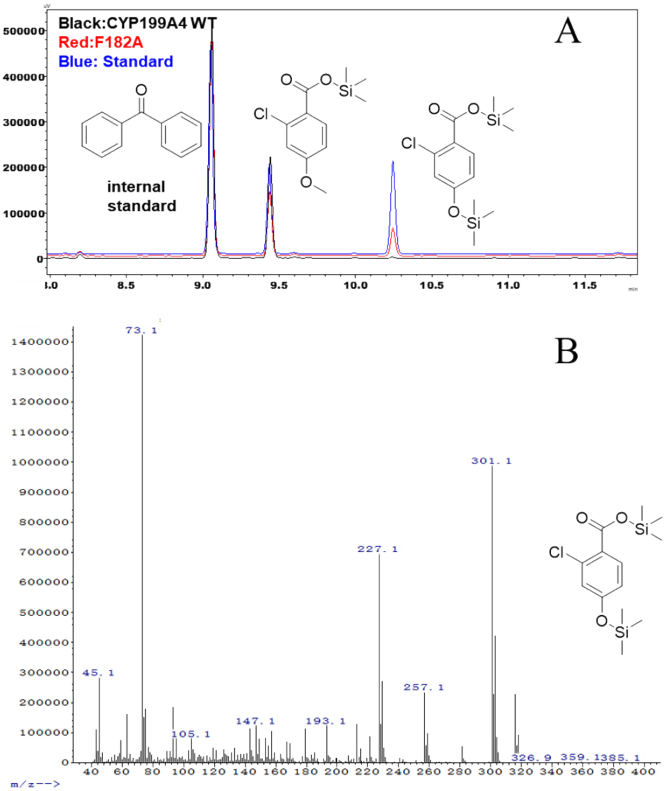

Figure S11. (A) GC analyses of the 60-minute reaction of 2-chloro-4-methoxybenzoic acid demethylation catalyzed by CYP199A4 WT and F182A (1 μM) at 30 °C in the presence of 10 mM H_2O_2. (B) GC-MS analyses for the product 2-chloro-4-hydroxybenzoic acid (derivatized m/z =316.1).

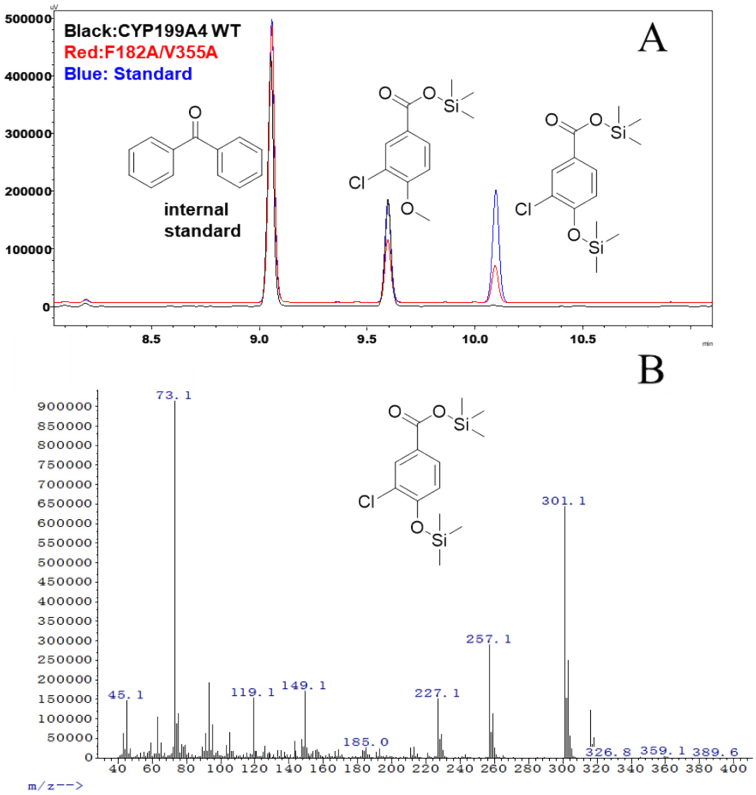

Figure S12. (A) GC analyses of the 60-minute reaction of 3-chloro-4-methoxybenzoic acid demethylation catalyzed by CYP199A4 WT and F182A/V355A (1 μM) at 30 °C in the presence of 10 mM H_2O_2. (B) GC-MS analyses for the product 3-chloro-4-hydroxybenzoic acid (derivatized m/z =316.1).

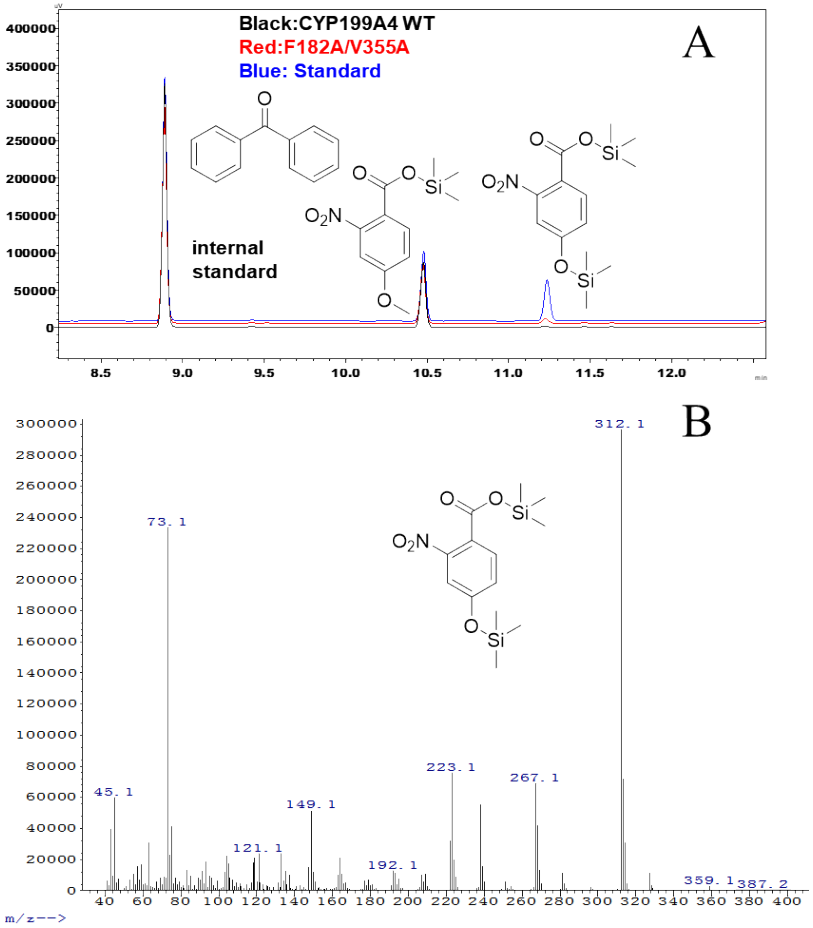

Figure S13. (A) GC analyses of the 60-minute reaction of 2-nitro-4-methoxybenzoic acid demethylation catalyzed by CYP199A4 WT and F182A/V355A (1 µM) at 30 °C in the presence of 10 mM H_2O_2. (B) GC-MS analyses for the product 2-nitro-4-hydroxybenzoic acid (derivatized m/z =327.1).

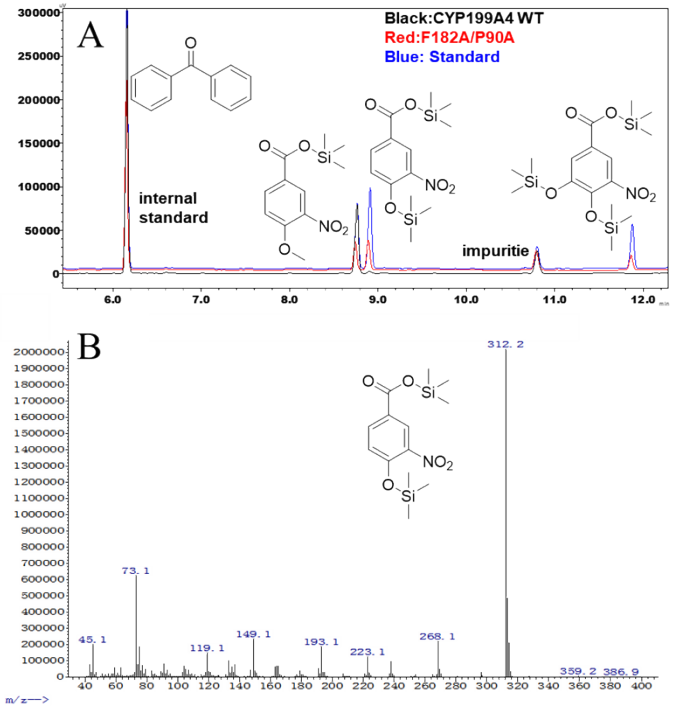

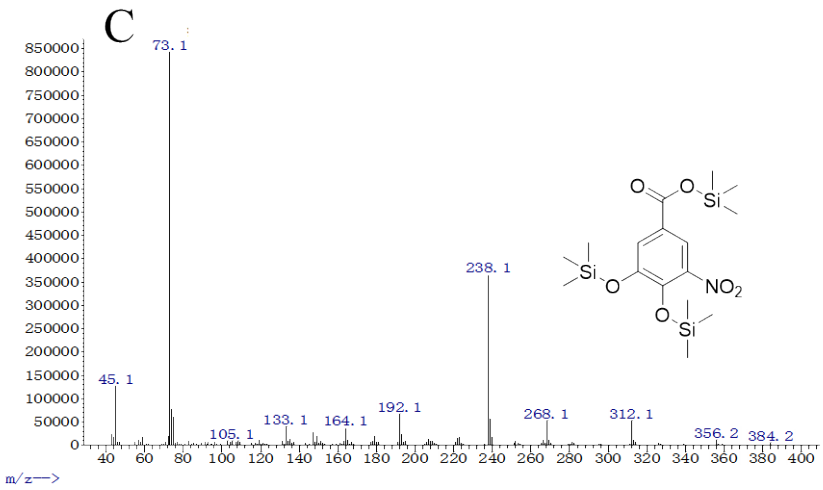

Figure S14. (A) GC analyses of the 60-minute reaction of 3-nitro-4-methoxybenzoic acid demethylation catalyzed by CYP199A4 WT and F182A/P90A (1 μM) at 30 °C in the presence of 10 mM H_2O_2. (B) GC-MS analyses for the product 3-nitro-4-hydroxybenzoic acid (derivatized MV=327.1), (C) GC-MS analyses for the product 3-nitro-4,5-dihydroxybenzoic acid (derivatized m/z =415.1).

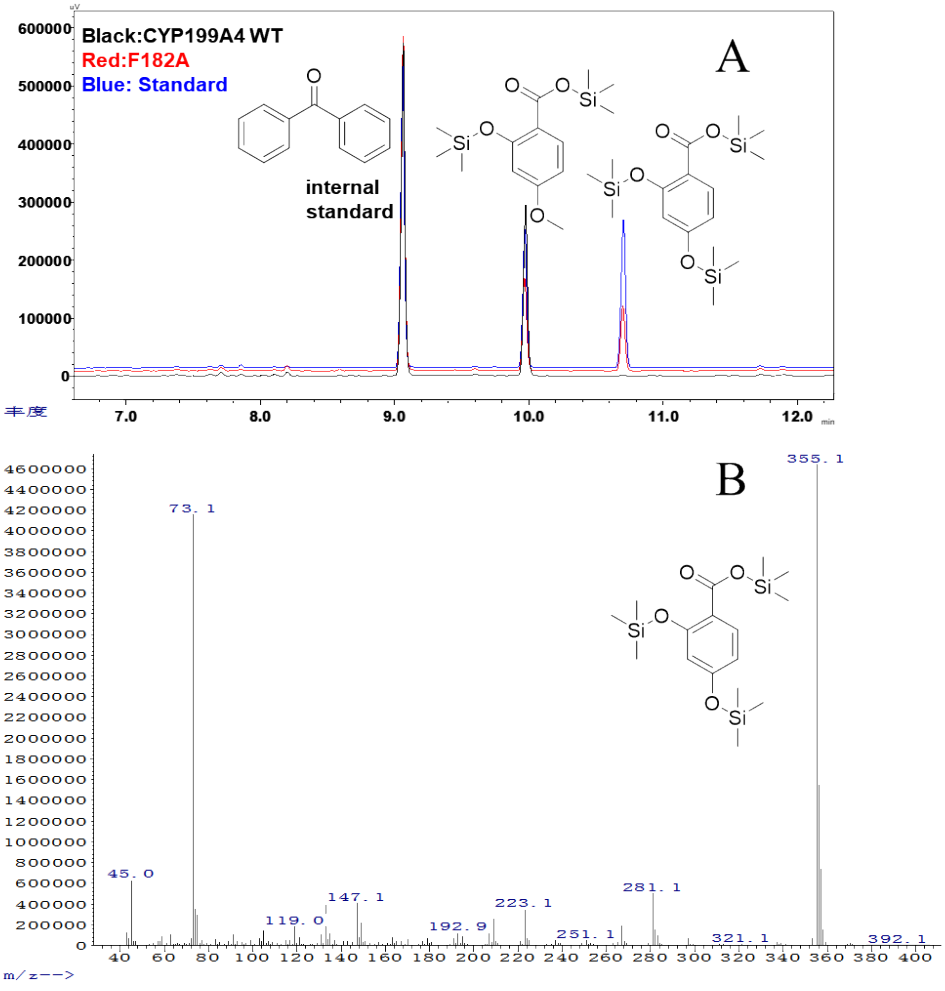

Figure S15. (A) GC analyses of the 60-minute reaction of 2-hydroxy-4-methoxybenzoic acid demethylation catalyzed by CYP199A4 WT and F182A (1 μM) at 30 °C in the presence of 10 mM H_2O_2. (B) GC-MS analyses for the product 2,4-dihydroxybenzoic acid (derivatized m/z =370.0).

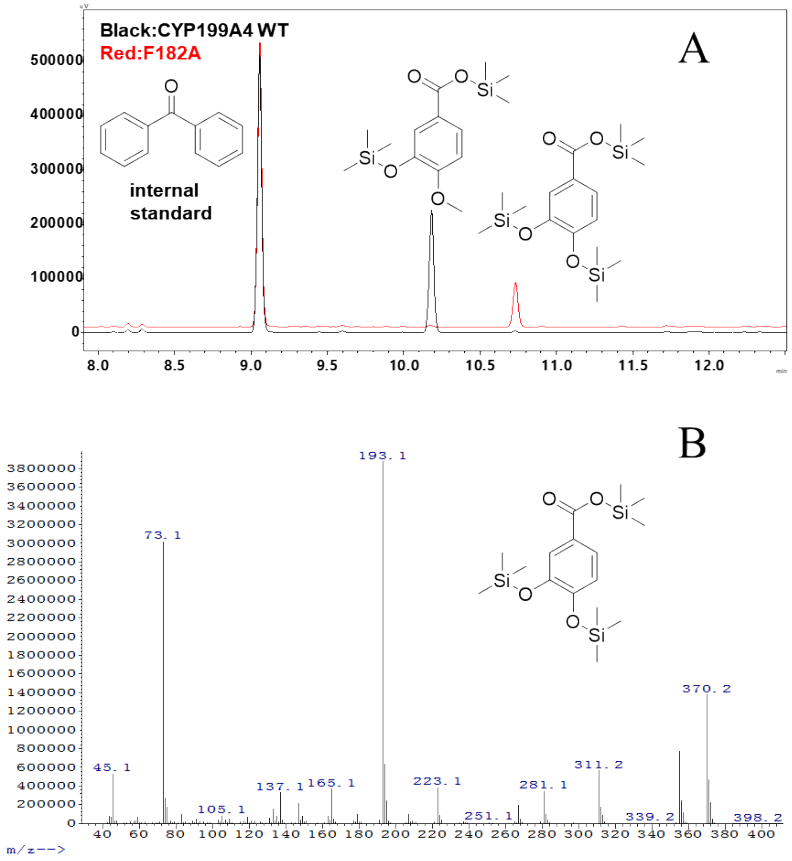

Figure S16. (A) GC analyses of the 60-minute reaction of 3-hydroxy-4-methoxybenzoic acid demethylation catalyzed by CYP199A4 WT and F182A (1 μM) at 30 °C in the presence of 10 mM H_2O_2. (B) GC-MS analyses for the product 3,4-dihydroxybenzoic acid (derivatized m/z =370.0).

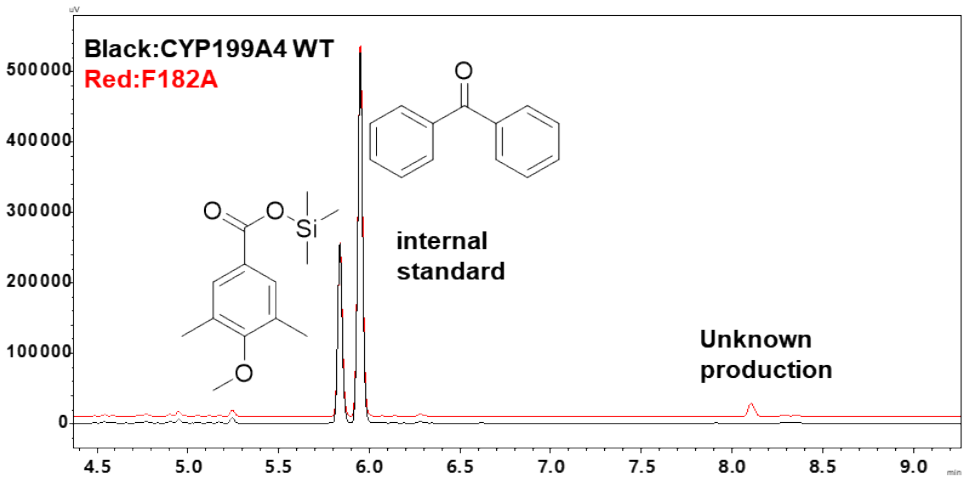

Figure S17. GC analyses of the 60-minute reaction of 3,5-dimethyl-4-methoxybenzoic acid catalyzed by CYP199A4 WT and F182A (1 μM) at 30 °C in the presence of 10 mM H_2O_2.

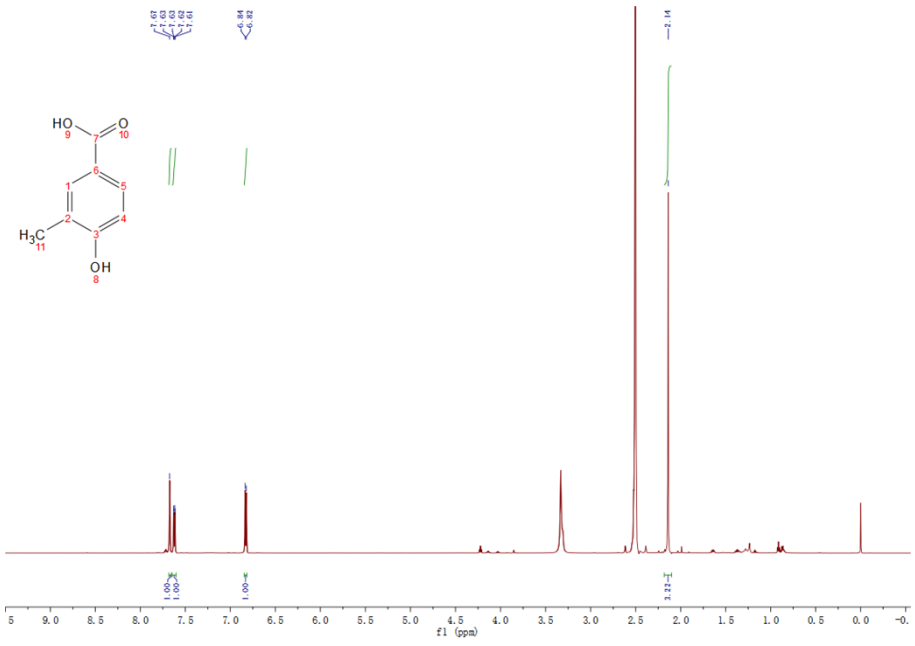

Figure S18. 1H-NMR spectrum to identify hydroxylation products of 3-methyl-4-methoxybenzoic acid. 1H 1H-NMR (600 MHz, DMSO-d6) δ 7.67 (S, 1H), 7.63-7.61 (m, 1H), 6.84-6.82 (d, J = 12 Hz, 2H), 2.14 (s, 3H).

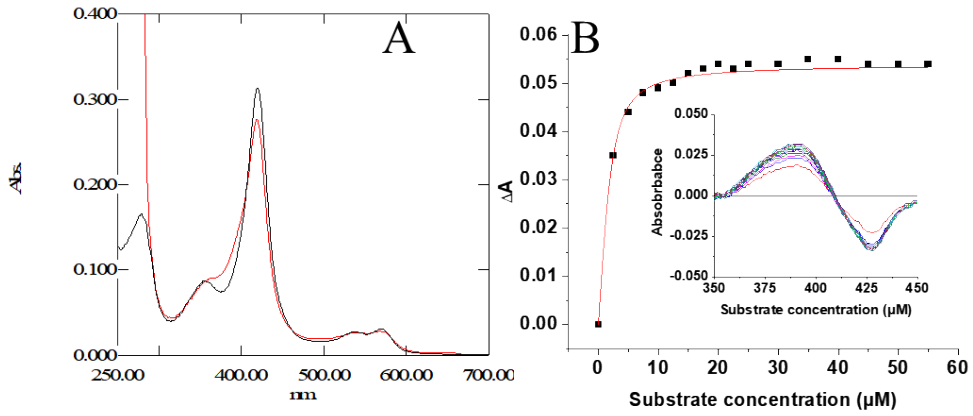

Figure S19. (A) Spin state shift of F182A (red; substrate-bound F182A, black; substrate-free F182A) with the substrates. (B) Substrate binding constant analysis of 4-methoxybenzoic acid (K_d=0.65 μM).

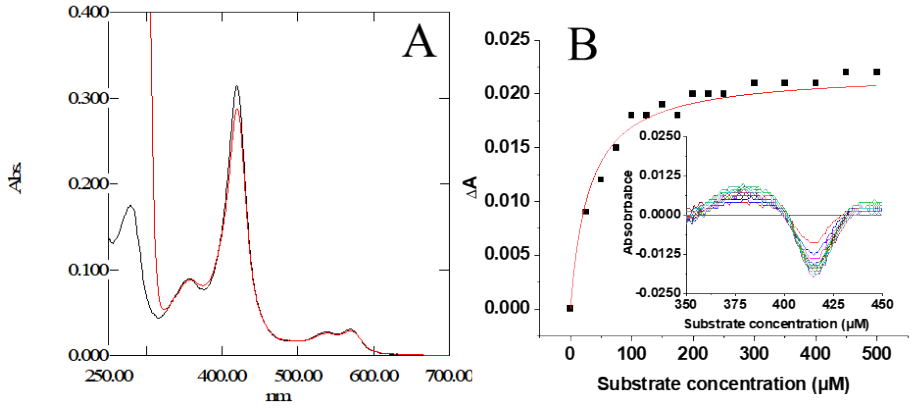

Figure S20. (A) Spin state shift of F182A (red; substrate-bound F182A, black; substrate-free F182A) with the substrates. (B) Substrate binding constant analysis of 3-methoxybenzoic acid (K_d =29.7 μM).

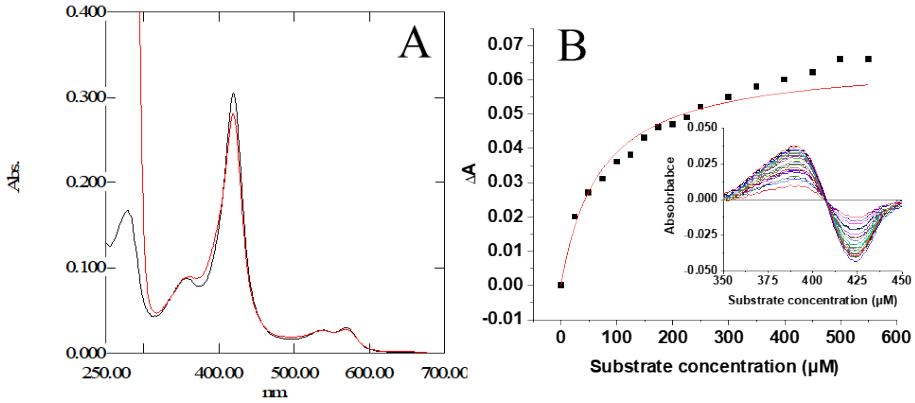

Figure S21. (A) Spin state shift of F182A (red; substrate-bound F182A, black; substrate-free F182A) with the substrates. (B) Substrate binding constant analysis of 2,4-dimethoxybenzoic acid (K_d =69.8 μM).

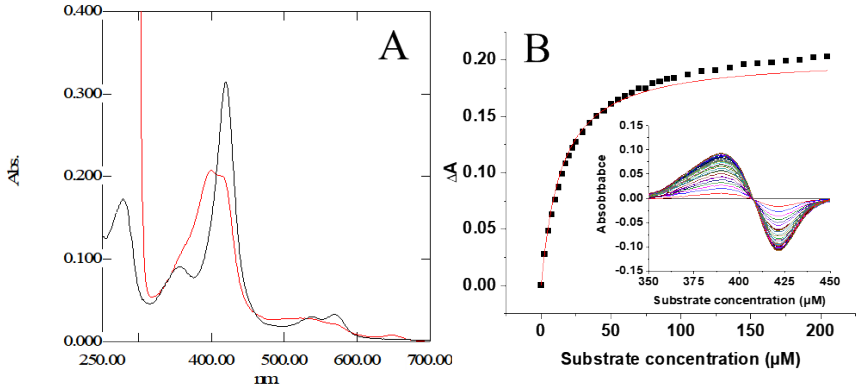

Figure S22. (A) Spin state shift of F182A (red; substrate-bound F182A, black; substrate-free F182A) with the substrates. (B) Substrate binding constant analysis of 3,4-dimethoxybenzoic acid (K_d =13.1 μM).

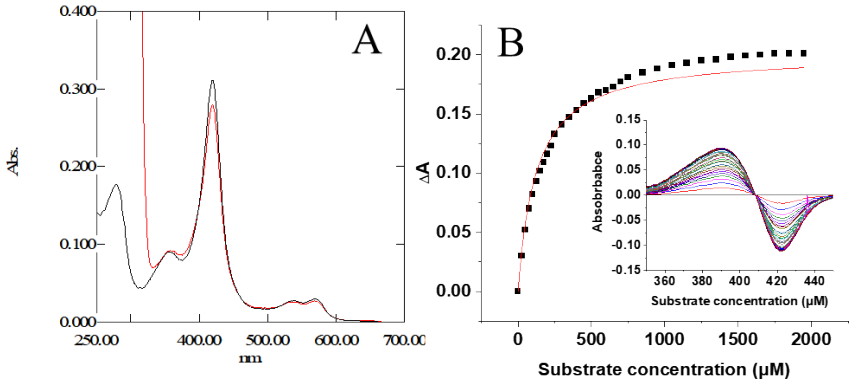

Figure S23. (A) Spin state shift of F182A (red; substrate-bound F182A, black; substrate-free F182A) with the substrates. (B) Substrate binding constant analysis of 3,5-dimethoxybenzoic acid (K_d=10.9 μM).

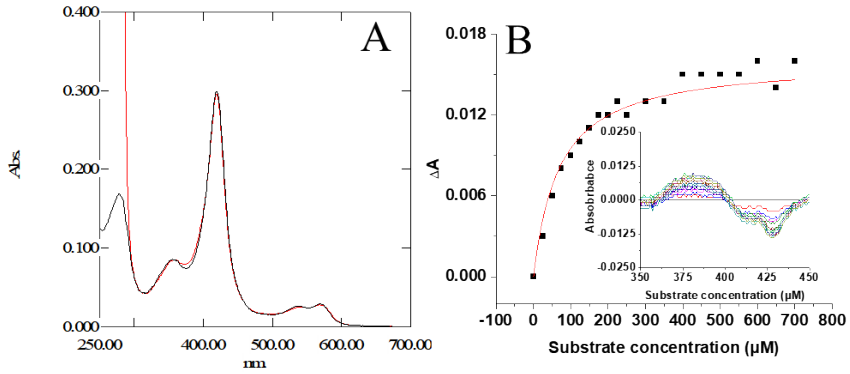

Figure S24. (A) Spin state shift of F182A (red; substrate-bound F182A, black; substrate-free F182A) with the substrates. (B) Substrate binding constant analysis of 2-methyl-4-methoxybenzoic acid (K_d =67.2 μM).

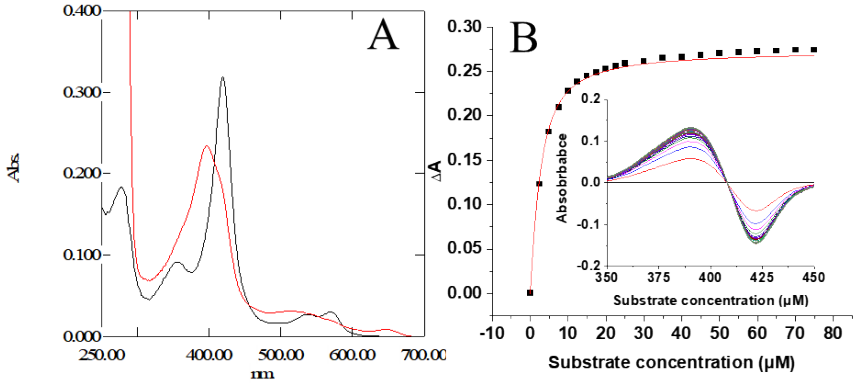

Figure S25. (A) Spin state shift of F182A (red; substrate-bound F182A, black; substrate-free F182A) with the substrates. (B) Substrate binding constant analysis of 3-methyl-4-methoxybenzoic acid (K_d =1.7 μM).

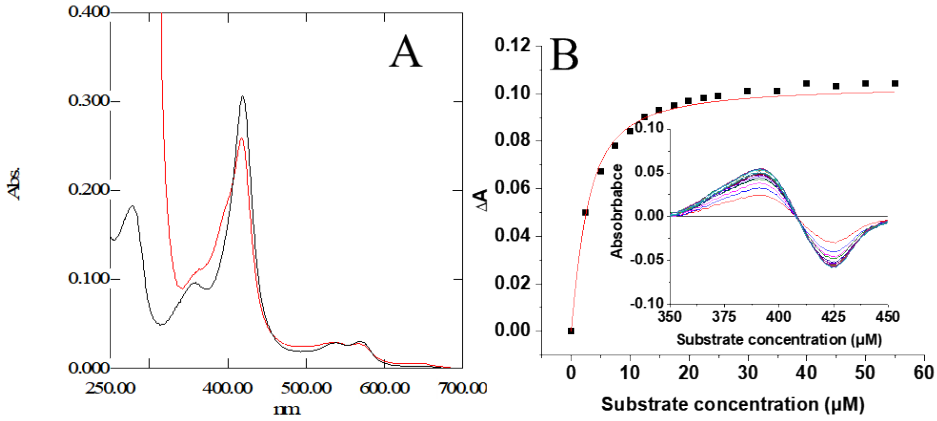

Figure S26. (A) Spin state shift of F182A (red; substrate-bound F182A, black; substrate-free F182A) with the substrates. (B) Substrate binding constant analysis of 2-hydroxy-4-methoxybenzoic acid (K_d =1.7 μM).

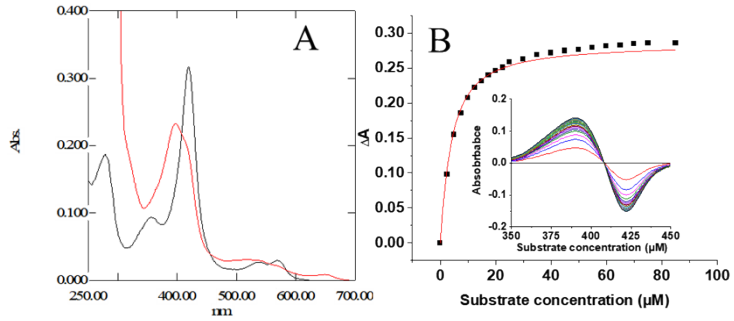

Figure S27. (A) Spin state shift of F182A (red; substrate-bound F182A, black; substrate-free F182A) with the substrates. (B) Substrate binding constant analysis of 3-hydroxy-4-methoxybenzoic acid (K_d =2.9 μM).

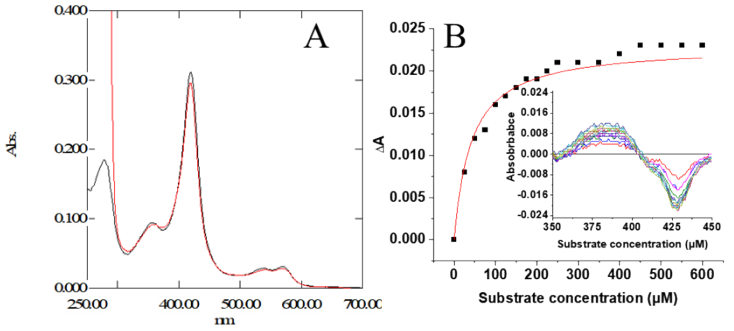

Figure S28. (A) Spin state shift of F182A (red; substrate-bound F182A, black; substrate-free F182A) with the substrates. (B) Substrate binding constant analysis of 2-chloro-4-methoxybenzoic acid (K_d =40.1 μM).

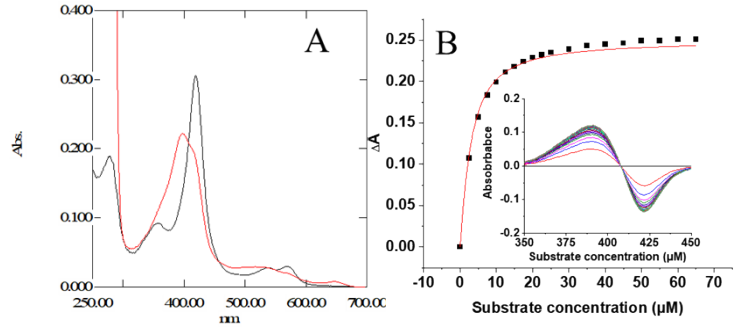

Figure S29. (A) Spin state shift of F182A (red; substrate-bound F182A, black; substrate-free F182A) with the substrates. (B) Substrate binding constant analysis of 3-chloro-4-methoxybenzoic acid (K_d =2.0 μM).

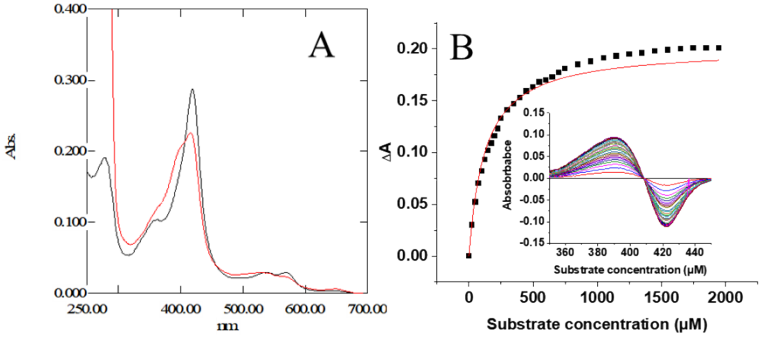

Figure S30. (A) Spin state shift of F182A (red; substrate-bound F182A, black; substrate-free F182A) with the substrates. (B) Substrate binding constant analysis of 3,5-dimethyl-4-methoxybenzoic acid (K_d =123.4 μM).

Supporting Tables

Table S1. Data collection and refinement statistics.[a]

Protein	CYP199A4 F182A
Ligand	4-methoxybenzoic acid
PDB Entry	**8WS4**
Data collection	
Space group	*P 1 21 1*
Unit cell dimensions	
a, b, c (Å)	44.674, 51.829, 78.959
α, β, γ (°)	90, 93.154, 90
Multiplicity	2.8 (1.6)
Completeness (%)	99.41 (98.08)
I/σ_I	7.4 (2.4)
R_{merge}	0.046 (0.383)
Wilson B factor (Å2)	14.18
CC1/2	0.998 (0.809)
Refinement	
Resolution range (Å)	30.38 - 1.53 (1.59 - 1.53)
NO. reflections	54232 (5315)
R_{work}/R_{free}	0.1547/0.1755
Number of non-hydrogen atoms	3591
Macromolecules	3052
Ligands/ions	58
Solvent	481
Average B-factor	19.57
Macromolecules	17.98
Ligands	14.06
Solvent	30.28
r.m.s.d. for ideal value	
Bond length (Å)	0.006
Bond angle (°)	0.90
Ramachandran plot	
Favored/allowed/outliers (%)	98.21/1.79/0

a Values for the highest resolution shell are given in parentheses.

Table S2. CYP199A4 mutants catalyzed 4-methoxybenzoic acid demethylation.[a]

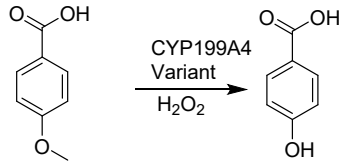

CYP199A4 variant	4-hydroxybenzoic acid TON
F182A	980±10
F182A/D251A	-
F182A/D251G	-
F182A/D251N	22±2
F182A/D251H	57±5
F182A/D251E	94±1

a Reaction conditions: CYP199A4 mutants (1 μM), 4-methoxybenzoic acid (2 mM 2 % DMSO), H_2O_2 (10 mM) in pH 7.4 Tris-HCl buffer at 30 °C. TON: Turnover numbers were estimated over a 60-min reaction.

Table S3. CYP199A4 mutants catalyzed 3-methoxybenzoic acid demethylation.[a]

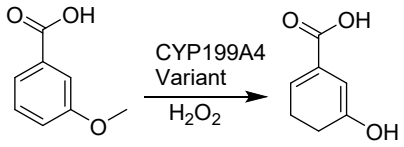

Enzymes	3-hydroxybenzoic acid TON
CYP199A4	-
F182A	104±3
F182A/F185A	18±1
F182A/S247G	76±5
F182A/F298S	54±1
F182A/V355A	70±2
F182A/K89A	89±3
F182A/P90A	108±2

a Reaction conditions: CYP199A4 mutants (1 μM), 3-methoxybenzoic acid (2 mM 2 % DMSO), H_2O_2 (10 mM,) in pH 7.4 Tris-HCl buffer at 30 °C. TON: Turnover numbers were estimated over a 60-min reaction.

Table S4. CYP199A4 mutants catalyzed 2,4-dimethoxybenzoic acid demethylation.[a]

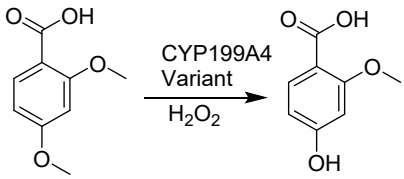

Enzymes	2-methoxy-4-hydroxybenzoic acid TON
CYP199A4	-
F182A	418±19
F182A/F185A	20±0
F182A/S247G	128±9
F182A/F298S	52±2
F182A/V355A	187±24
F182A/K89A	101±5
F182A/P90A	15±1

a Reaction conditions: CYP199A4 mutants (1 μM), 2,4-dimethoxybenzoic acid (2 mM 2 % DMSO), H_2O_2 (10 mM) in pH 7.4 Tris-HCl buffer at 30 °C. TON: Turnover numbers were estimated over a 60-min reaction.

Table S5. CYP199A4 mutants catalyzed 3,4-dimethoxybenzoic acid demethylation.[a]

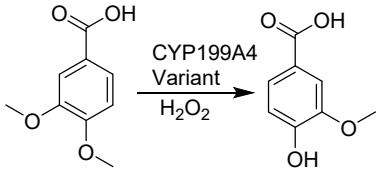

Enzymes	3-methoxy-4-hydroxybenzoic acid TON
CYP199A4	-
F182A	742±28
F182A/F185A	34±0
F182A/S247G	114±7
F182A/F298S	679±67
F182A/V355A	836±19
F182A/P71G	181±1
F182A/K89A	423±35
F182A/P90A	499±16

a Reaction conditions: CYP199A4 mutants (1 μM), 3,4-dimethoxybenzoic acid (2 mM 2 % DMSO), H_2O_2 (10 mM) in pH 7.4 Tris-HCl buffer at 30 °C. TON: Turnover numbers were estimated over a 60-min reaction.

Table S6. CYP199A4 mutants catalyzed 3,5-dimethoxybenzoic acid demethylation.[a]

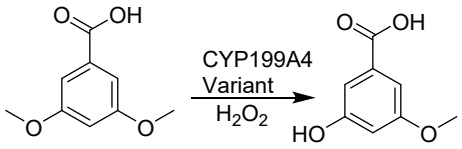

Enzymes	3-hydroxy-5-methoxybenzoic acid TON
CYP199A4	-
F182A	266±0
F182A/F185A	-
F182A/S247G	191±8
F182A/F298S	60±0
F182A/V355A	201±0
F182A/K89A	159±2
F182A/P90A	97±3

a Reaction conditions: CYP199A4 mutants (1 μM), 3,5-dimethoxybenzoic acid (2 mM 2 % DMSO), H_2O_2 (10 mM) in pH 7.4 Tris-HCl buffer at 30 °C. TON: Turnover numbers were estimated over a 60-min reaction.

Table S7. CYP199A4 mutants catalyzed 2-methyl-4-methoxybenzoic acid demethylation.[a]

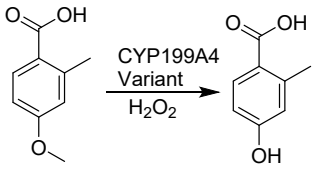

Enzymes	2-methyl-4-hydroxybenzoic acid TON
CYP199A4	32±1
F182A	645±1
F182A/F185A	20±1
F182A/S247G	84±2
F182A/F298S	217±11
F182A/V355A	512±1
F182A/K89A	293±4
F182A/P90A	202±5

a Reaction conditions: CYP199A4 mutants (1 μM), 2-methyl-4-methoxybenzoic (2 mM 2 % DMSO), H_2O_2 (10 mM) in pH 7.4 Tris-HCl buffer at 30 °C. TON: Turnover numbers were estimated over a 60-min reaction.

Table S8. CYP199A4 mutants catalyzed 3-methyl-4-methoxybenzoic acid demethylation.[a]

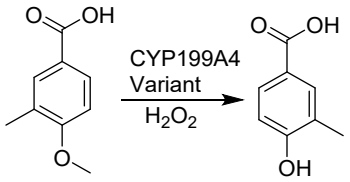

Enzymes	3-methyl-4-hydroxybenzoic acid TON
CYP199A4	65±2
F182A	1282±9
F182A/F185A	204±2
F182A/S247G	293±9
F182A/F298S	892±20
F182A/V355A	1290±15
F182A/K89A	679±16
F182A/P90A	1062±18

a Reaction conditions: CYP199A4 mutants (1 μM), 3-methyl-4-methoxybenzoic (2 mM 2 % DMSO), H_2O_2 (10 mM) in pH 7.4 Tris-HCl buffer at 30 °C. TON: Turnover numbers were estimated over a 60-min reaction.

Table S9. CYP199A4 mutants catalyzed 2-hydroxy-4-methoxybenzoic acid demethylation.[a]

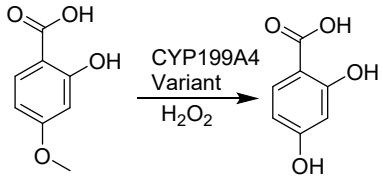

Enzymes	2,4-dihydroxybenzoic acid TON
CYP199A4	17±0
F182A	747±16
F182A/F185A	58±3
F182A/S247G	73±9
F182A/F298S	437±13
F182A/V355A	570±14
F182A/K89A	321±28
F182A/P90A	386±30

a Reaction conditions: CYP199A4 mutants (1 μM), 2-hydroxy-4-methoxybenzoic (2 mM 2 % DMSO), H_2O_2 (10 mM) in pH 7.4 Tris-HCl buffer at 30 °C. TON: Turnover numbers were estimated over a 60-min reaction.

Table S10. CYP199A4 mutants catalyzed 3-hydroxy-4-methoxybenzoic acid demethylation.[a]

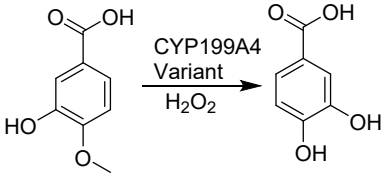

Enzyme	3,4-dihydroxybenzoic acid TON
CYP199A4	30±0
F182A	724±32
F182A/F185A	72±0
F182A/S247G	397±24
F182A/F298S	683±42
F182A/V355A	1023±15
F182A/K89A	692±35
F182A/P90A	932±12

a Reaction conditions: CYP199A4 mutants (1 μM), 3-hydroxy-4-methoxybenzoic (2 mM 2 % DMSO), H_2O_2 (10 mM) in pH 7.4 Tris-HCl buffer at 30 °C. TON: Turnover numbers were estimated over a 60-min reaction.

Table S11. CYP199A4 mutants catalyzed 2-chloro-4-methoxybenzoic acid demethylation.[a]

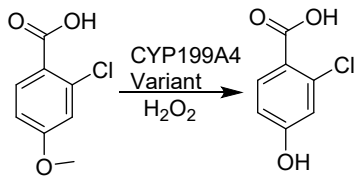

Enzymes	2-chloro-4-hydroxybenzoic acid TON
CYP199A4	31±2
F182A	565±10
F182A/F185A	13±0
F182A/S247G	88±2
F182A/F298S	129±10
F182A/V355A	424±10
F182A/K89A	230±10
F182A/P90A	198±2

a Reaction conditions: CYP199A4 mutants (1 μM), 2-chloro-4-methoxybenzoic acid (2 mM 2 % DMSO), H_2O_2 (10 mM) in pH 7.4 Tris-HCl buffer at 30 °C. TON: Turnover numbers were estimated over a 60-min reaction.

Table S12. CYP199A4 mutants catalyzed 3-chloro-4-methoxybenzoic acid demethylation.[a]

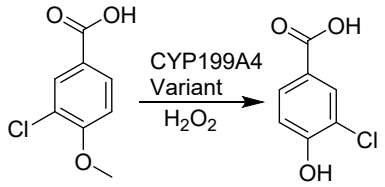

Enzymes	3-chloro-4-hydroxybenzoic acid TON
CYP199A4	42±2
F182A	629±10
F182A/F185A	185±7
F182A/S247G	276±7
F182A/F298S	634±3
F182A/V355A	680±13
F182A/K89A	653±23
F182A/P90A	780±7

a Reaction conditions: CYP199A4 mutants (1 μM), 3-chloro-4-methoxybenzoic acid (2 mM 2 % DMSO), H_2O_2 (10 mM) in pH 7.4 Tris-HCl buffer at 30 °C. TON: Turnover numbers were estimated over a 60-min reaction.

Table S13. CYP199A4 mutants catalyzed 2-nitro-4-methoxybenzoic acid demethylation.[a]

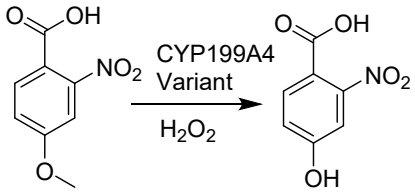

Enzyme	2-nitro-4-methoxybenzoic acid TON
CYP199A4	71±2
F182A	162±8
F182A/F185A	19±3
F182A/S247G	119±1
F182A/F298S	121±1
F182A/V355A	165±7
F182A/K89A	159±2
F182A/P90A	124±14

a Reaction conditions: CYP199A4 mutants (1 μM), 2-nitro-4-methoxybenzoic (2 mM 2 % DMSO), H_2O_2 (10 mM) in pH 7.4 Tris-HCl buffer at 30 °C. TON: Turnover numbers were estimated over a 60-min reaction.

Table S14. CYP199A4 mutants catalyzed 3-nitro-4-methoxybenzoic acid demethylation.[a]

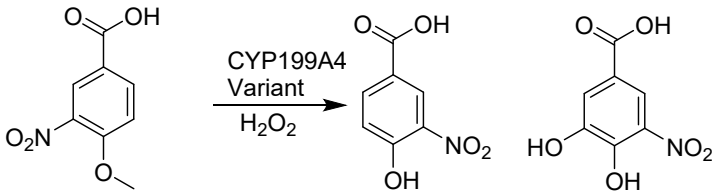

Enzyme	3-nitro-4-methoxybenzoic acid TON	4,5-dihydroxy-3-nitrobenzoic acid TON
CYP199A4	73±8	-
F182A	484±32	57±8
F182A/F185A	211±3	-
F182A/S247G	220±6	78±3
F182A/F298S	410±2	-
F182A/V355A	584±26	68±6
F182A/K89A	749±95	98±9
F182A/P90A	926±99	416±59

a Reaction conditions: CYP199A4 mutants (1 μM), 3-nitro-4-methoxybenzoic (2 mM 2 % DMSO), H_2O_2 (10 mM) in pH 7.4 Tris-HCl buffer at 30 °C. TON: Turnover numbers were estimated over a 60-min reaction.

References

1. I. Matsunaga, A. Ueda, T. Sumimoto, K. Ichihara, M. Ayata and H. Ogura, *Arch Biochem Biophys*, 2001, **394**, 45-53.
2. Z. J. Wang, H. Renata, N. E. Peck, C. C. Farwell, P. S. Coelho and F. H. Arnold, *Angew. Chem. Int. Ed.*, 2014, **53**, 6810-6813.
3. P. Zhao, F. Kong, Y. Jiang, X. Qin, X. Tian and Z. Cong, *J Am Chem Soc*, 2023, **145**, 5506-5511.
4. T. Omura, R. Sato, *J Biol Chem,* 1964**, *239***, 2379-2385..
5. F. Yu, Q. Wang, M. Li, H. Zhou, K. Liu, K. Zhang, Z. Wang, Q. Xu, C. Xu, Q. Pan and J. He, *J Appl Crystallogr*, 2019, **52**, 472-477.
6. P. D. Adams, P. V. Afonine, G. Bunkoczi, V. B. Chen, I. W. Davis, N. Echols, J. J. Headd, L. W. Hung, G. J. Kapral, R. W. Grosse-Kunstleve, A. J. McCoy, N. W. Moriarty, R. Oeffner, R. J. Read, D. C. Richardson, J. S. Richardson, T. C. Terwilliger and P. H. Zwart, *Acta Crystallogr D Biol Crystallogr*, 2010, **66**, 213-221.
7. P. Emsley, B. Lohkamp, W. G. Scott and K. Cowtan, *Acta Crystallogr D Biol Crystallogr*, 2010, **66**, 486-501.
8. N. Echols, N. W. Moriarty, H. E. Klei, P. V. Afonine, G. Bunkoczi, J. J. Headd, A. J. McCoy, R. D. Oeffner, R. J. Read, T. C. Terwilliger and P. D. Adams, *Acta Crystallogr D Biol Crystallogr*, 2014, **70**, 144-154.
9. V. B. Chen, W. B. Arendall, 3rd, J. J. Headd, D. A. Keedy, R. M. Immormino, G. J. Kapral, L. W. Murray, J. S. Richardson and D. C. Richardson, *Acta Crystallogr D Biol Crystallogr*, 2010, **66**, 12-21.
10. J. C. Gordon, J. B. Myers, T. Folta, V. Shoja, L. S. Heath and A. Onufriev, *Nucleic Acids Res*, 2005, **33**, W368-371.
11. R. Anandakrishnan, B. Aguilar and A. V. Onufriev, *Nucleic Acids Res*, 2012, **40**, W537-541.
12. D. Van Der Spoel, E. Lindahl, B. Hess, G. Groenhof, A. E. Mark and H. J. Berendsen, *J Comput Chem*, 2005, **26**, 1701-1718.
13. C. Tian, K. Kasavajhala, K. A. A. Belfon, L. Raguette, H. Huang, A. N. Migues, J. Bickel, Y. Wang, J. Pincay, Q. Wu and C. Simmerling, *J Chem Theory Comput*, 2020, **16**, 528-552.
14. F. Neese, *WIRES Comput Mol Sci*, 2022, **12**.
15. T. Lu and F. Chen, *J Comput Chem*, 2012, **33**, 580-592.
16. D. A. Case, T. E. Cheatham, 3rd, T. Darden, H. Gohlke, R. Luo, K. M. Merz, Jr., A. Onufriev, C. Simmerling, B. Wang and R. J. Woods, *J Comput Chem*, 2005, **26**, 1668-1688.
17. R. Salomon-Ferrer, D. A. Case and R. C. Walker, *WIRES Comput Mol Sci*, 2012, **3**, 198-210.
18. A. K. Rappé, C. J. Casewit, K. S. Colwell, III. Goddard, W. M. Skiff, *J Comput Chem* 1992, **114 (25)**, 10024-10035.
19. S. Miyamoto, P.A. Kollman, *J Comput Chem* 1992, **13 (8)**, 952-962.
20. B. Hess, H. Bekker, H. J. C. Berendsen, J. G. E. M. Fraaije, *J Comput Chem*, 1997, **18 (12)**, 1463-1472..
21. T. Darden, D. York and L. Pedersen, *J Chem Phys*, 1993, **98**, 10089-10092.
22. A. S. Lemak and N. K. Balabaev, *Mol. Simul.*, 1994, **13**, 177-187.
23. M. Parrinello and A. Rahman, *J Appl Phys*, 1981, **52**, 7182-7190.
24. J. Kästner, *WIREs Comput Mol Sci*, 2011, **1**, 932-942.
25. S. Kumar, J. M. Rosenberg, D. Bouzida, R. H. Swendsen and P. A. Kollman, *J Comput Chem*, 1992, **13**, 1011-1021.
26. G. P. Bienert**.** F. Chaumont, *Method Enzymol.,*2014, **1840 (5)**, 1596-1604 .